

Article

Mapping the Potential Global Distribution of Red Imported Fire Ant (*Solenopsis invicta* Buren) Based on a Machine Learning Method

Shuai Chen ^{1,2,†} , Fangyu Ding ^{1,2,†}, Mengmeng Hao ^{1,2,*} and Dong Jiang ^{1,2,3,*} 

¹ State Key Laboratory of Resources and Environmental Information Systems, Institute of Geographical Sciences and Natural Resources Research, Chinese Academy of Sciences, Beijing 100101, China; chenshuai17@mails.ucas.ac.cn (S.C.); dingfy.17b@igsnr.ac.cn (F.D.)

² College of Resource and Environment, University of Chinese Academy of Sciences, Beijing 100049, China

³ Key Laboratory of Carrying Capacity Assessment for Resource and Environment, Ministry of Land & Resources, Beijing 100101, China

* Correspondence: haomm@igsnr.ac.cn (M.H.); jiangd@igsnr.ac.cn (D.J.); Tel.: +86-10-64889433 (M.H.); +86-10-64889433 (D.J.)

† These authors contributed equally to this work.

Received: 19 October 2020; Accepted: 3 December 2020; Published: 6 December 2020



Abstract: As one of the most notorious invasive species, the red imported fire ant (*Solenopsis invicta* Buren) has many adverse impacts on biodiversity, environment, agriculture, and human health. Mapping the potential global distribution of *S. invicta* becomes increasingly important for the prevention and control of its invasion. By combining the most comprehensive occurrence records with an advanced machine learning method and a variety of geographical, climatic, and human factors, we have produced the potential global distribution maps of *S. invicta* at a spatial resolution of $5 \times 5 \text{ km}^2$. The results revealed that the potential distribution areas of *S. invicta* were primarily concentrated in southeastern North America, large parts of South America, East and Southeast Asia, and Central Africa. The deforested areas in Central Africa and the Indo-China Peninsula were particularly at risk from *S. invicta* invasion. In addition, this study found that human factors such as nighttime light and urban accessibility made considerable contributions to the boosted regression tree (BRT) model. The results provided valuable insights into the formulation of quarantine policies and prevention measures.

Keywords: *S. invicta*; red imported fire ant; potential distribution; boosted regression tree; human factors

1. Introduction

Biological invasion is a global problem, causing serious environmental, economic, and social damages [1,2]. Included in “100 of the World’s Worst Invasive Alien Species” [3], the red imported fire ant (*Solenopsis invicta* Buren) is recognized as one of the most widespread and damaging invasive pests known to impact ecosystem processes, agricultural production, infrastructure, and human health [4–9]. *S. invicta* is native to South America and was accidentally introduced into the United States in the 1930s [10,11]. In subsequent years, this species rapidly spread throughout California and other regions of the world, including the Caribbean islands, Australia, New Zealand, Japan, China, and South Korea [12–16]. Given the strong adaptive and reproductive capacity, *S. invicta* has great potential to colonize numerous other regions, inflicting enormous damage to the local economy and ecosystems [17,18]. Prevention of biological invasion is much less expensive than post-entry control.

Hence, it is essential to study the potential global distribution of *S. invicta* to provide a scientific basis for the formulation of prevention and control measures.

Species distribution models (SDMs) have been widely used in predicting the potential geographic distribution of *S. invicta* (Table 1). For example, Killion et al. applied a colony-growth model to examine the potential range of *S. invicta* in the United States by incorporating temperature-driven development rates of *S. invicta* life-stages and simulating the number of workers in a colony [19]. Korzukhin et al. formulated a dynamic model of colony growth and alate production on the assumption that soil temperature was the key ecological factor determining colony growth and reproduction to predict the current extreme distributions and future range of *S. invicta* in the United States [20]. Morrison et al. superimposed precipitation data upon the temperature-based predictions to estimate colony alate production and predicted the future global geographic range limits of *S. invicta* at the station scale [21]. Sutherst and Maywald used the CLIMEX model to estimate the response of *S. invicta* to temperature and moisture from its range in the United States and estimated the potential global areas at risk for *S. invicta* invasion [14]. Ward modelled the potential geographic distribution of six invasive ant species in New Zealand by three different methods (BIOCLIM, DOMAIN, and Maxent) with 19 bioclimatic variables [22]. Ulrichs et al. predicted *S. invicta* distributions with climate (relative humidity, temperature, and precipitation) and habitat data (landcover type) [23]. More recently, Wang et al. quantified colony growth based on daily air temperature and precipitation data, to simulate the potential range of *S. invicta* in China under current and future climate conditions [24]. Sung et al. modelled the potential distribution of *S. invicta* under current climate conditions using six different species distribution models combined with 19 bioclimatic variables, and selected the random forest (RF) model to obtain its potential global distribution under climate change [13].

Table 1. Summary of existing literature on predicting the potential geographic distribution of *S. invicta*.

Author/Year	Methods	Environmental Variables	Extent	Resolution
Killion et al., 1993 [19]	Colony-growth model	Temperature	The United States	-
Korzukhin et al., 2001 [20]	Colony-growth model	Temperature, precipitation	The United States	Station
Morrison et al., 2004 [21]	Colony-growth model	Temperature, precipitation	Global	Station
Sutherst et al., 2005 [14]	CLIMEX	Temperature, moisture	Global	10' (~340 km ²)
Ward, 2007 [22]	BIOCLIM, DOMAIN, MAXENT	19 bioclimatic variables	New Zealand	30" (~1 km ²)
Ulrichs et al., 2008 [23]	Stepwise Discriminant function analysis	Relative humidity, temperature, precipitation, landcover type	the United States	2.5' (~85 km ²)
Wang et al., 2018 [24]	colony-growth model	Temperature, precipitation	China	0.1° (~10 km ²)
Sung et al., 2018 [13]	GLM, GAM, MARS, ANN, CTA, RF	5 bioclimatic variables	Global	30" (~1 km ²)

Numerous studies have indicated that biological invasion is often closely associated with human impacts [25–28]. Human activities such as trade, tourism, and transport are indispensable indicators that determine the potential range of invasive species [29]. *S. invicta* is more likely to colonize disturbed environments of human-associated habitats [22,30–32], and the cross-regional spread is often aided by human transportation [33,34]. However, existing studies focus on the impact of climatic factors on the distribution of *S. invicta*, whereas few of them take human factors into account during modelling. Besides, the occurrence localities of *S. invicta* used in existing studies are relatively limited, and few studies predict the global potential distribution of *S. invicta* on a high spatial resolution. Therefore, the main purposes of this study are to (1) Fully collect the location records of *S. invicta*. (2) Comprehensively analyze the climatic, geographical, and human factors that may influence the distribution of *S. invicta* and quantitatively simulate the relationship between each type of factors and *S. invicta* presence with a machine learning method-the boosted regression tree (BRT). (3) Predict the global potential distribution of *S. invicta* at a spatial resolution of 5×5 km².

2. Materials and Methods

2.1. Data

2.1.1. Environmental Variables

The geographical distribution of *S. invicta* is influenced by many environmental factors. In the present study, these factors were divided into three categories: climatic factors, geographical factors, and human factors.

Climatic factors such as temperature and precipitation are the main constraints that limit the distribution and growth of *S. invicta*. For example, continental areas where the annual precipitation is less than 510 mm, cannot provide a suitable habitat for *S. invicta* [21,35,36], and its overwintering population is confined by the minimum temperature of the winter season [37,38]. Previous studies have also indicated that the foraging activity and colony growth of *S. invicta* have remarkable relations with temperature and humidity [30,39–41]. Therefore, we adopted accumulated annual precipitation, maximum temperature, minimum temperature, and relative humidity to reflect the climatic conditions.

Geographical factors also play a substantial role in determining the distribution of *S. invicta*. *S. invicta* is well adapted to opportunistic exploitation of disturbed habitats and some extreme environments [42]. For instance, in arid continental areas, *S. invicta* will be able to successfully establish if there are permanent sources of water (i.e., lakes, rivers, or dams) or regularly irrigated areas (i.e., fields or lawns) [11,21]. Additionally, some studies have indicated that *S. invicta* prefers open, sunny areas while it is less abundant in densely wooded areas [30,43]. Thus, the data of distance to a river, distance to lake, and distance to ocean [44] were adopted to reflect the water availability, the normalized difference vegetation index (NDVI) data was applied to reflect the density of vegetation cover, and the elevation dataset was used to reflect the temperature variance with altitude.

Human activities and urbanization are crucial factors that affect the distribution and abundance of ant species [45–47]. *S. invicta* may look for sanctuary in human habitations or infrastructure (such as climate-controlled buildings or greenhouses) in areas where the cold climate makes it difficult to overwinter [14]. The natural dispersal distances are usually limited to hundreds of meters or a few kilometers [30], while long-distance dispersal occurs primarily through human activities or major disturbances [22,32]. Commercial transportation of agricultural or landscaping materials (e.g., containers, equipment, or potted plants soil) has resulted in the cross-regional spread of *S. invicta* colonies [30,34]. Land cover type, population density, and nighttime light were obtained to represent the extent of human activities. The urban accessibility dataset, for estimating the travel time to major cities, was used to reflect the connectivity of different locations and the concentration of economic activity.

The environmental variables used for this study were received in a gridded format with various resolutions. To ensure the spatial consistency of these variables, we converted the spatial resolutions of all variable data to 0.05 degrees (approximately 5 km). Detailed information on the related spatial variables used in this study is shown in Table 2.

Table 2. The environmental variables adopted in this study.

Category	Predictor Variables	Data Source
Climatic factors	Maximum temperature Minimum temperature Relative humidity Accumulated annual precipitation	CliMond Climate Data [48]
Geographical factors	Distance to ocean Distance to river Distance to lake Elevation Vegetation	G-Econ 4.0 dataset of Yale University [44] Shuttle Radar Topography Mission (SRTM) [49] Global Inventory Modelling and Mapping Studies (GIMMS) group [50]
Human factors	Land cover Urban accessibility Population density Nighttime light	Global Land Cover-SHARE (GLC-SHARE) [51] European Commission Joint Research Center [52] NASA Socioeconomic Data and Applications Center (SEDAC) [53] Earth Observation Group, NOAA [54]

2.1.2. Presence Data

In this study, the occurrence localities of *S. invicta* were derived from various sources, including websites, literature, field surveys, and government reports. *S. invicta* occurrence records with detailed geographical coordinate information were downloaded from the website of the Global Biodiversity Information Facility (GBIF) [55], supplemented by AntWeb [56] and Centre for Agriculture and Bioscience International (CABI) [57]. Published studies and maps of *S. invicta* occurrences were also applied to extract the location information of *S. invicta*. Also, in this study, we used data from JK Wetterer's records to document the worldwide range of *S. invicta* until 2013, including both published and unpublished [58]. The occurrence records from the literature published after 2013 were included as well, as shown in Table S1 (see supplementary materials).

In addition, according to the "List of administrative areas for the distribution of agricultural plant quarantine pests in China 2019", 387 counties in 12 provinces of China have been invaded by *S. invicta* [59]. Since the occurrence was recorded at the county scale, the county centroids were used as the occurrence locations. To obtain more localities of *S. invicta* occurrence in China, we went to Fujian Province to conduct field surveys and collected the locations of nests of *S. invicta*.

After deduplication, a total of 1610 occurrence records of *S. invicta* were collected, as shown in Figure 1. The occurrence records of *S. invicta* from websites and literature were mainly located in North and South America, whereas records from field surveys and government reports were mostly distributed in China.

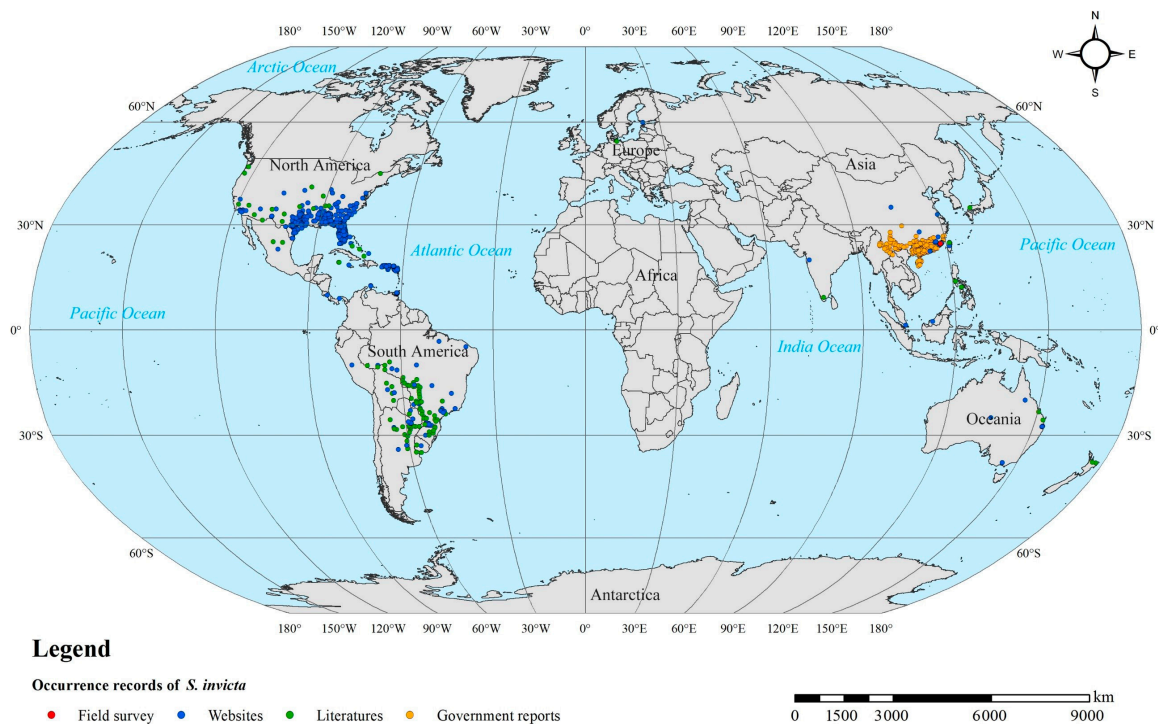


Figure 1. Global occurrence records of *S. invicta*.

2.1.3. Pseudo-Absence Data

Pseudo-absences (PAs), also known as background data, are widely used in species distribution modelling when only presence data is available. As the selection of PAs could severely impact the model performance, different strategies have been proposed to improve the selection of appropriate PAs. One of the methods is to randomly select PAs from all points outside a pre-defined region based on a simple preliminary model or based on a minimum distance to the presence. Barbet-Massin et al. showed that this method performed better in machine learning methods (i.e., BRT and RF), and recommended using the same number of PAs as available presences [60]. In this study, we derived PAs with environmental

exclusion based on prior knowledge from studies of Killion et al. [19] and Korzukhin et al. [20]. Their studies applied colony-growth models which incorporated temperature and precipitation (in Korzukhin et al. [20]) to identify the potential range of *S. invicta*. The estimated annual precipitation (510 mm) and annual minimum temperature (-17.8 °C) were applied as reasonable thresholds that limit the range expansion for *S. invicta*. By setting environmental limits, PAs are selected outside the suitable area of the species to keep a certain distance from the presence points.

Besides, water and iced bodies were also excluded from PAs selection by overlaying with the land cover map. To reduce the effect of sample selection bias on the model prediction, we implemented the selection of PAs 300 times randomly. After each random selection process, we constructed 3220 samples (1610 presences and 1610 PAs) and divided the samples into two subsets, the training samples and validation samples accounted for 75% (2415) and 25% (805) of the total samples respectively.

2.2. Boosted Regression Tree Model

In this study, a machine learning method, the boosted regression tree (BRT) model, was adopted to predict the potential global distribution of *S. invicta*. BRT is a combination of statistical and machine learning techniques. It has been widely used in species distribution modelling [61–64]. BRT combines the advantages of both regression trees and boosting algorithms. The characteristics from the tree-based methods give the BRT abilities to deal with different types of predictor variables (numeric, categorical, binary, etc.), accommodating missing data, and being insensitive to outliers [65,66]. In addition, the model can fit complex nonlinear relationships as well as identifying and modelling the interactions between different predictors automatically. Based on the idea that it is easier to find and compute an average from many rough rules than to find a single highly accurate prediction rule, the boosting technique combines many simple tree models to improve the performance and predictive accuracy of single tree models [65]. Boosting implements a forward and stepwise procedure to merge results of several competing models, where tree models are fitted interactively to a subset of the training data, using appropriate methods (stochastic gradient descent here) gradually to increase emphasis on observations that were modelled poorly by the existing collection of trees.

Based on the above-mentioned reasons, the BRT model was applied in the present study. The R version 3.3.3 statistical programming environment [67] was used in combination with the extension packages (i.e., *dismo* [68], *caret* [69], and *gbm* [70]) to build the BRT model and evaluate the prediction accuracy. The optimal settings of the BRT models were determined by the cross-validation results from 300 times repeated computations. The learning rate determines the contribution of each tree to the growing model, the tree complexity controls whether interactions are fitted and the bag fraction determines the proportion of the used training data. The main tuning parameters were set as follows (*tree.complexity* = 4, *learning.rate* = 0.005, *bag.fraction* = 0.75, *step.size* = 10, *cv.folds* = 10, *max.trees* =), and the other parameters were kept as *gbm* defaults. Following these steps, we fitted an ensemble of 300 BRT models to increase the robustness of the model prediction and quantify the model uncertainty.

3. Results

3.1. Accuracy Evaluation

A ten-fold cross-validation method was applied to each model to avoid overfitting, and the area under the curve (AUC) statistic and true skill statistic (TSS) were used to evaluate the predictive performances of the BRT models. The validation statistics suggested that the ensemble BRT model performed well. The AUC values for the training dataset and validation dataset were $0.981(\pm 0.004)$ and $0.981(\pm 0.009)$ respectively, and the TSS were 0.879 for the training dataset and 0.853 for the validation dataset, which indicated a high predictive accuracy. In addition, the model uncertainty was also quantified in the spatial predictions based on the standard deviation values across the model ensemble. The uncertainty analysis revealed that the prediction uncertainty in most areas was low

(lower than 0.26), and high uncertainty areas were mostly distributed around high-risk areas for *S. invicta* infestation (Figure 2).

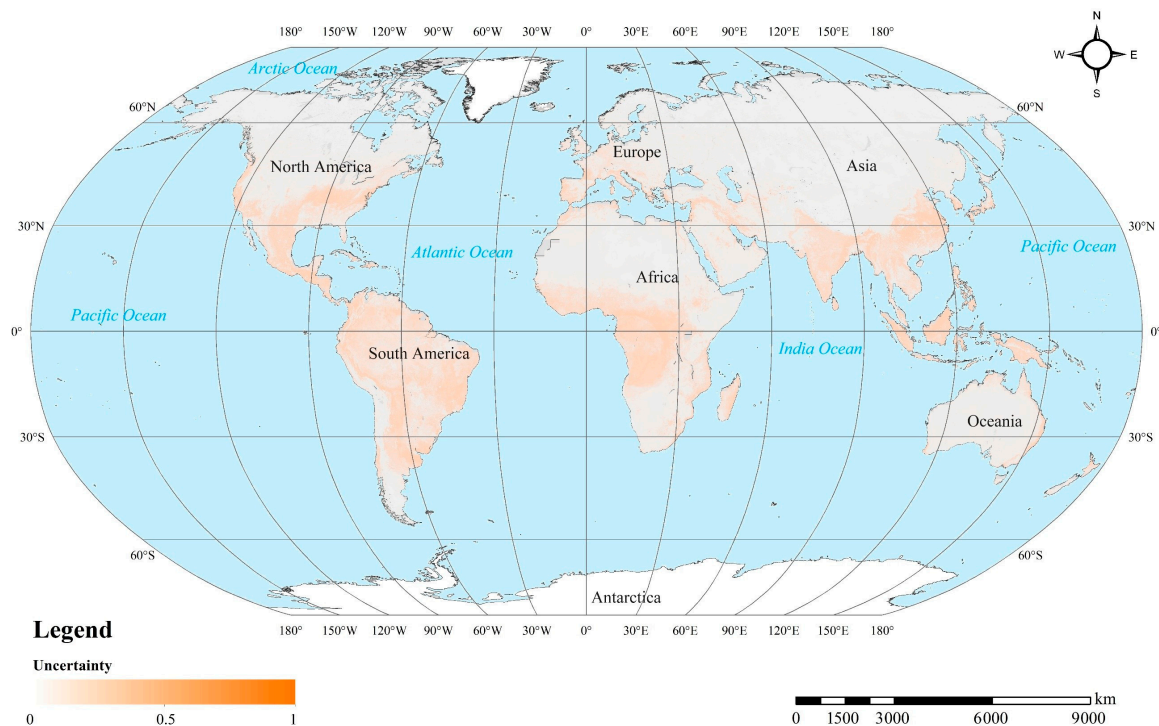


Figure 2. Uncertainty distribution of the BRT model.

3.2. Potential Risk of *S. Invicta* Invasion

On the foundation of the observed relationship between *S. invicta* occurrence records and each environment predictor, we used the fitted ensemble BRT models to predict the global infestation risk of *S. invicta*. Figure 3 shows the infestation risk level, also considered as the suitability of *S. invicta*, on a continuous scale from 0 to 1, which was generated by calculating the mean prediction across all models for each grid cell. The predicted infestation risk map revealed that the high-risk areas are primarily concentrated in medium and low latitude regions, including southeastern North America, large parts of South America, East and Southeast Asia, and Central Africa, which were consistent with the current distribution range of the species. The predicted medium-risk areas were distributed around the high-risk areas.

In North America, the predicted high-risk areas were mainly distributed in the southeast and west coast of the United States, the east coast of Mexico, northern Guatemala, and northern Belize (Figure S1). In South America, the potential areas suitable for *S. invicta* were located in most parts, including Brazil, Colombia, Venezuela, Guyana, Suriname, French Guiana, eastern Peru, northeastern Bolivia, western Paraguay, northeastern Argentina, and Uruguay (Figure S2). The suitable areas in Europe were scattered around the Mediterranean, in coastal regions of Portugal, Spain, France, Italy, Albania, and Greece (Figure S3). In Africa, the suitable areas were mainly concentrated in Central Africa, including southern Cameroon, Equatorial Guinea, Gabon, western Angola, Congo, midwestern DR Congo as well as some coastal cities in Ivory Coast, Ghana, Benin, Nigeria, and South Africa (Figure S4). In Asia, the predicted high-risk areas were mainly distributed in East Asia, Southeast Asia, and coastal South Asia, specifically including southern China, Indo-China Peninsula (i.e., Burma, Laos, Thailand, Cambodia, and Vietnam), Malaysia, northern Philippines, and Bangladesh. Coastal areas in India, Indonesia, South Korea, and Japan were also medium or high-risk areas (Figure S5). In Oceania, the southeastern coast of Australia, northern New Zealand, and coastal Papua New Guinea were at medium risk (Figure S6). It is noteworthy that in both Central Africa and Southeast Asia (particularly

on Indo-China Peninsula), though there were no or very few records of previous *S. invicta* presence, the model predicted high risk in these regions. Also, in some coastal areas and islands of Central America, the Mediterranean, Oceania, the Indian Ocean, and Southeast Asia, the model also predicted medium- or high-risk for *S. invicta* infestation.

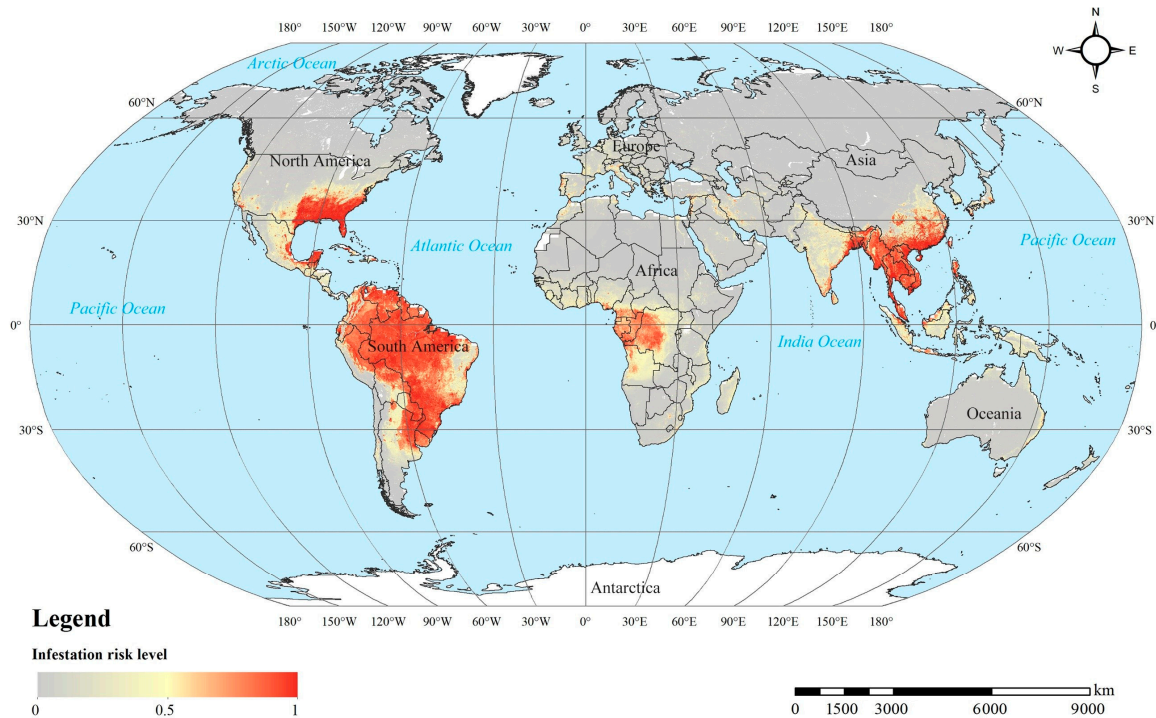


Figure 3. Global infestation risk level of *S. invicta*.

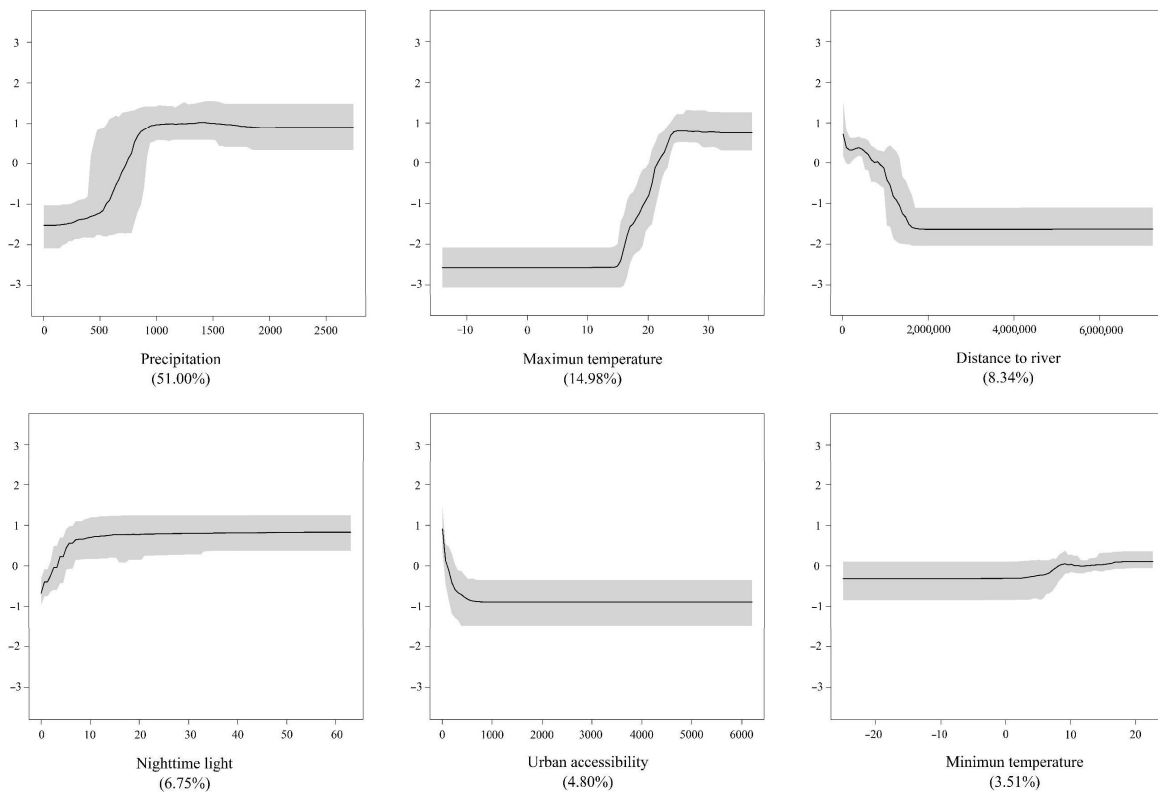
3.3. Relative Contribution of Environmental Factors

To identify the key factors that determine the potential distribution of *S. invicta*, we quantified the contribution of each predictor to the ensemble BRT model using the relative contribution (RC) indicator (Table 3). The statistics suggested that the climatic factors accounting for 71.14% of the variation explained by the ensemble BRT models, were the most important predictors in the model, followed by human factors (15.55%) and geographical factors (13.31%). Accumulated annual precipitation was the most significant predictor, with a relative contribution rate of 51% ($\pm 7.21\%$), followed by the maximum temperature, which had a relative contribution of 14.98% ($\pm 4.44\%$). The distance to a river, nighttime light, and urban accessibility had relative contributions of 8.34% ($\pm 2.33\%$), 6.75% ($\pm 3.24\%$), and 4.8% ($\pm 2.22\%$), respectively. The contribution rates of other predictors are shown in Table 3.

As illustrated in Figure 4, the accumulated annual precipitation was positively correlated to the probability of suitable land for *S. invicta*, an increase in the probability was observed as the accumulated annual precipitation initially increased from 500 mm. The maximum temperature and nighttime light also showed a positive correlation with suitability, whereas the distance to a river, urban accessibility presented a negative correlation with suitability, and for the minimum temperature, the correlation was not significant.

Table 3. The relative contribution of the related environmental factors.

	Mean Relative Importance (%)	Standard Deviation (%)
Climatic factors	71.14%	-
Accumulated annual precipitation	51.00%	7.21%
Maximum temperature	14.98%	4.44%
Minimum temperature	3.51%	1.97%
Relative humidity	1.65%	0.81%
Human factors	15.55%	-
Nighttime light	6.75%	3.24%
Urban accessibility	4.80%	2.22%
Land cover	2.30%	0.75%
Population density	1.70%	0.74%
Geographical factors	13.31%	-
Distance to river	8.34%	2.33%
Vegetation	2.24%	0.84%
Elevation	1.52%	0.91%
Distance to lake	0.69%	0.46%
Distance to ocean	0.52%	0.29%

**Figure 4.** Marginal effect plots of main spatial predictors overall 300 boosted regression tree (BRT) ensembles fitted to the full data set. The black lines depict the mean effect curves, and the shaded areas represent the 95% confidence interval.

4. Discussion

The results were consistent with *S. invicta*'s current range and the predictions of previous studies [13,14,21], and our study presented more details and finer distinctions with a higher resolution. The potential suitable areas for *S. invicta* were primarily concentrated in southeastern North America, large parts of South America, East and Southeast Asia, and Central Africa. This was also in line with the predictions of the Maxent model (see Figure S7). By comparison with the potential distribution

of the black imported fire ant (*Solenopsis richteri*), a closely related species to *S. invicta*, we found that *S. richteri* was able to survive in higher latitude than *S. invicta*. *S. richteri* had broader potential in temperate regions such as Europe, East Asia, South Africa, and eastern North America [71]. By contrast, *S. invicta* was more abundant in Southeast Asia, Central Africa, and northern South America. This was largely because *S. richteri* is more tolerant to cold than *S. invicta*, while *S. invicta* has higher tolerance to heat and desiccation stresses than *S. richteri*.

These maps could be used to identify areas where *S. invicta* could establish but has yet to be reported or areas where the infestation risk is underestimated. For example, in Central Africa and Indo-China Peninsula, though *S. invicta* has rarely been observed or reported before, the BRT model predicted high-risks for *S. invicta* infestation. It is worth noting that the geographical distribution range of these high-risk areas overlapped with that of tropical rainforests. Many studies suggest that *S. invicta* constructs earthen mounds in the open, sunny areas for brood thermoregulation and is less abundant in the warm, wet, and dense forests [21,42,72]. Therefore, it is more likely to establish in those disturbed and developed forested areas, including the edges of forests or agricultural areas [73], deforested areas are especially in danger of becoming colonized. According to the “Global Ecosystems and Environment Observation and Analysis Annual Report 2019” [74], forest coverage decreased in both Central Africa and Indo-China Peninsula from 2000 to 2018, largely as a result of devastating forests for arable land [75,76]. The deforested areas could provide suitable habitats for the establishment of *S. invicta*, and should be taken into adequate account. In addition, the model also predicted medium- or high-risk in some coastal areas and islands of Central America, the Mediterranean, Oceania, the Indian Ocean, and Southeast Asia, where the ecological environment is relatively fragile, the introduction of *S. invicta* may cause devastating damage to local species and biodiversity. Therefore, inspection and quarantine measures in these medium- or high-risk areas need to be strengthened, thereby preventing it from becoming widespread, and minimizing the ecological and economic impacts.

Climatic variables were the most important factors responsible for the environmental suitability of *S. invicta*. Precipitation and temperature are the major determinants that limit the distribution range of *S. invicta*. The low minimum temperature in the winter, the high maximum temperature in the summer, or inadequate precipitation would prevent it from becoming successfully established. As illustrated in Figure 4, when the accumulated annual precipitation increased from 500 mm and the maximum temperature increased from 15 °C, the habitat suitability for *S. invicta* also increased, which conform to the ecological characteristics of the species [40,77,78]. As the survival of *S. invicta* in arid regions is highly dependent on sources of permanent water or irrigated areas, the distance to a river also made considerable contributions to the BRT model. The suitability gradually decreased as the distance to a river increased. It is encouraging that human factors also had a strong influence on the model prediction with a total contribution of 15.55%. Nighttime light and urban accessibility appeared to be important human factors determining the potential distribution of *S. invicta*. Specifically, the environmental suitability for *S. invicta* increased as the nighttime light index rose (which indicates a high degree of human activities). This may reflect its preference for human disturbances, *S. invicta* has been shown to inhabit a wide variety of human habitats and infrastructures [30–32]. The urban accessibility factor is negatively correlated with suitability. When the travel time to major cities increased (which represents lower connectivity and less economic activity), the environmental suitability for *S. invicta* decreased. These results added credibility to the rationality of the initial assumption that human activities may provide *S. invicta* with suitable living conditions and promote its spread.

It should be noted that the potential distribution of *S. invicta* is also affected by many other factors. For example, soil properties, flooding, and the distribution of food resources, natural enemies, and host plants may also affect the distribution of *S. invicta* [30,31,79–81], future prediction could be refined by including more comprehensive factors and higher spatio-temporal resolution datasets.

5. Conclusions

In this study, we combined the most comprehensive occurrence records with an advanced machine learning method and a variety of variables to predict the potential global distribution of *S. invicta*. Our results indicated that the potential distribution areas of *S. invicta* were primarily concentrated in southeastern North America, large parts of South America, East and Southeast Asia, and Central Africa. The deforested areas in Central Africa and the Indo-China Peninsula were especially at risk from *S. invicta* invasion. Some islands and coastal areas in Central America, the Mediterranean, Oceania, the Indian Ocean, and Southeast Asia were also found to be suitable habitats for *S. invicta*. These findings could provide a scientific basis to formulate prevention and control measures proactively. Additionally, human factors such as nighttime light and urban accessibility made considerable contributions to the BRT model, this could provide an important baseline for incorporating human factors in modelling the potential distribution of *S. invicta* as well as other species.

Supplementary Materials: The following are available online at <http://www.mdpi.com/2071-1050/12/23/10182/s1>, Table S1: Location records of *S. invicta* from literatures published after 2013, Figure S1: Occurrence points and infestation risk level of *S. invicta* in North America, Figure S2: Occurrence points and infestation risk level of *S. invicta* in South America, Figure S3: Occurrence points and infestation risk level of *S. invicta* in Europe, Figure S4: Occurrence points and infestation risk level of *S. invicta* in Africa, Figure S5: Occurrence points and infestation risk level of *S. invicta* in Asia, Figure S6: Occurrence points and infestation risk level of *S. invicta* in Oceania, Figure S7: Global infestation risk level of *S. invicta* predicted by Maxent, Figure S8: Sampling points of *S. invicta* field survey, Figure S9: Sampling points pictures of *S. invicta* field survey.

Author Contributions: Conceptualization, M.H. and D.J.; Data curation, S.C. and F.D.; Formal analysis, S.C.; Investigation, S.C.; Methodology, M.H., D.J. and F.D.; Resources, S.C., M.H. and D.J.; Software, F.D.; Supervision, M.H. and D.J.; Validation, F.D.; Visualization, S.C.; Writing—original draft, S.C.; Writing—review & editing, M.H., D.J. and F.D. All authors have read and agreed to the published version of the manuscript.

Funding: This research was funded by the Strategic Priority Research Program of the Chinese Academy of Sciences, grant number XDA20010203.

Acknowledgments: We thank Yushu Qian for providing valuable suggestions.

Conflicts of Interest: The authors declare no conflict of interest.

References

1. Pejchar, L.; Mooney, H.A. Invasive species, ecosystem services and human well-being. *Trends Ecol. Evol.* **2009**, *24*, 497–504. [[CrossRef](#)] [[PubMed](#)]
2. Mooney, H.A.; Cleland, E.E. The evolutionary impact of invasive species. *Proc. Natl. Acad. Sci. USA* **2001**, *98*, 5446–5451. [[CrossRef](#)] [[PubMed](#)]
3. Lowe, S.; Browne, M.; Boudjelas, S.; de Poorter, M. *100 of the World's Worst Invasive Alien Species: A Selection from the Global Invasive Species Database*; Invasive Species Specialist Group: Auckland, New Zealand, 2000; Volume 12.
4. Adams, C.; Banks, W.; Lofgren, C.; Smittle, B.; Harlan, D. Impact of the red imported fire ant, *Solenopsis invicta* (Hymenoptera: Formicidae), on the growth and yield of soybeans. *J. Econ. Entomol.* **1983**, *76*, 1129–1132. [[CrossRef](#)]
5. Allen, C.R.; Epperson, D.; Garmestani, A. Red imported fire ant impacts on wildlife: A decade of research. *Am. Midl. Nat.* **2004**, *152*, 88–104. [[CrossRef](#)]
6. Gutrich, J.J.; VanGelder, E.; Loope, L. Potential economic impact of introduction and spread of the red imported fire ant, *Solenopsis invicta*, in Hawaii. *Environ. Sci. Policy* **2007**, *10*, 685–696. [[CrossRef](#)]
7. Jemal, A.; Hugh-Jones, M. A review of the red imported fire ant (*Solenopsis invicta* Buren) and its impacts on plant, animal, and human health. *Prev. Vet. Med.* **1993**, *17*, 19–32. [[CrossRef](#)]
8. Vinson, S.B. Impact of the invasion of the imported fire ant. *Insect Sci.* **2013**, *20*, 439–455. [[CrossRef](#)]
9. Wojcik, D.P.; Allen, C.R.; Brenner, R.J.; Forys, E.A.; Jouvenaz, D.P.; Lutz, R.S. Red Imported Fire Ants: Impact On Biodiversity. *Am. Entomol.* **2001**, *47*, 16–23. [[CrossRef](#)]
10. Callcott, A.-M.A.; Collins, H.L. Invasion and range expansion of imported fire ants (Hymenoptera: Formicidae) in North America from 1918–1995. *Fla. Entomol.* **1996**, *79*, 240–251. [[CrossRef](#)]

11. Vinson, S.B. Invasion of the red imported fire ant (*Hymenoptera: Formicidae*): Spread, biology, and impact. *Am. Entomol.* **1997**, *43*, 23–39. [[CrossRef](#)]
12. Davis, L.R., Jr.; van der Meer, R.K.; Porter, S.D. Red imported fire ants expand their range across the West Indies. *Fla. Entomol.* **2001**, *84*, 735. [[CrossRef](#)]
13. Sung, S.; Kwon, Y.S.; Lee, D.K.; Cho, Y. Predicting the potential distribution of an invasive species, *Solenopsis invicta* Buren (*Hymenoptera: Formicidae*), under climate change using species distribution models. *Entomol. Res.* **2018**, *48*, 505–513. [[CrossRef](#)]
14. Sutherst, R.W.; Maywald, G. A climate model of the red imported fire ant, *Solenopsis invicta* Buren (*Hymenoptera: Formicidae*): Implications for invasion of new regions, particularly Oceania. *Environ. Entomol.* **2005**, *34*, 317–335. [[CrossRef](#)]
15. Zeng, L.; Lu, Y.; He, X.; Zhang, W.; Liang, G. Identification of red imported fire ant *Solenopsis invicta* to invade mainland China and infestation in Wuchuan, Guangdong. *Entomol. Knowl.* **2005**, *42*, 144–148.
16. Zhang, R.; Li, Y.; Liu, N.; Porter, S.D. An overview of the red imported fire ant (*Hymenoptera: Formicidae*) in mainland China. *Fla. Entomol.* **2007**, *90*, 723–732. [[CrossRef](#)]
17. Williams, D.F.; Collins, H.L.; Oi, D.H. The red imported fire ant (*Hymenoptera: Formicidae*): An historical perspective of treatment programs and the development of chemical baits for control. *Am. Entomol.* **2001**, *47*, 146–159. [[CrossRef](#)]
18. Ross, K.G.; Shoemaker, D.D. Estimation of the number of founders of an invasive pest insect population: The fire ant *Solenopsis invicta* in the USA. *Proc. R. Soc. B Biol. Sci.* **2008**, *275*, 2231–2240. [[CrossRef](#)]
19. Killion, M.J.; Grant, W.E. A colony-growth model for the imported fire ant—Potential geographic range of an invading species. *Ecol. Model.* **1995**, *77*, 73–84. [[CrossRef](#)]
20. Korzukhin, M.D.; Porter, S.D.; Thompson, L.C.; Wiley, S. Modeling temperature-dependent range limits for the fire ant *Solenopsis invicta* (*Hymenoptera: Formicidae*) in the United States. *Environ. Entomol.* **2001**, *30*, 645–655. [[CrossRef](#)]
21. Morrison, L.W.; Porter, S.D.; Daniels, E.; Korzukhin, M.D. Potential global range expansion of the invasive fire ant, *Solenopsis invicta*. *Biol. Invasions* **2004**, *6*, 183–191. [[CrossRef](#)]
22. Ward, D.F. Modelling the potential geographic distribution of invasive ant species in New Zealand. *Biol. Invasions* **2007**, *9*, 723–735. [[CrossRef](#)]
23. Ulrichs, C.; Hopper, K.R. Predicting insect distributions from climate and habitat data. *Biocontrol* **2008**, *53*, 881–894. [[CrossRef](#)]
24. Wang, H.J.; Wang, H.; Tao, Z.X.; Ge, Q.S. Potential range expansion of the red imported fire ant (*Solenopsis invicta*) in China under climate change. *J. Geogr. Sci.* **2018**, *28*, 1965–1974.
25. Brown, J.H.; Sax, D.F. An essay on some topics concerning invasive species. *Austral. Ecol.* **2004**, *29*, 530–536. [[CrossRef](#)]
26. Crowl, T.A.; Crist, T.O.; Parmenter, R.R.; Belovsky, G.; Lugo, A.E. The spread of invasive species and infectious disease as drivers of ecosystem change. *Front. Ecol. Environ.* **2008**, *6*, 238–246. [[CrossRef](#)]
27. Di Marco, M.; Santini, L. Human pressures predict species' geographic range size better than biological traits. *Glob. Change Biol.* **2015**, *21*, 2169–2178. [[CrossRef](#)]
28. Roura-Pascual, N.; Hui, C.; Ikeda, T.; Leday, G.; Richardson, D.M.; Carpintero, S.; Espadaler, X.; Gómez, C.; Guénard, B.; Hartley, S. Relative roles of climatic suitability and anthropogenic influence in determining the pattern of spread in a global invader. *Proc. Natl. Acad. Sci. USA* **2011**, *108*, 220–225. [[CrossRef](#)]
29. Gallardo, B.; Zieritz, A.; Aldridge, D.C. The importance of the human footprint in shaping the global distribution of terrestrial, freshwater and marine invaders. *PLoS ONE* **2015**, *10*, e0125801. [[CrossRef](#)]
30. Rosson, J.L. Abiotic and Biotic Factors Affecting The Distribution of *Solenopsis invicta* Buren, *Brachymyrmex* sp., and *Linepithema humile* (Mayr) in East Baton Rouge Parish, Louisiana. Master Thesis, Louisiana State University, Baton Rouge, LA, USA, 2004.
31. King, J.R.; Tschinkel, W.R. Experimental evidence that human impacts drive fire ant invasions and ecological change. *Proc. Natl. Acad. Sci. USA* **2008**, *105*, 20339–20343. [[CrossRef](#)]
32. Bertelsmeier, C.; Luque, G.M.; Hoffmann, B.D.; Courchamp, F. Worldwide ant invasions under climate change. *Biodivers. Conserv.* **2015**, *24*, 117–128. [[CrossRef](#)]
33. Suarez, A.V.; Holway, D.A.; Case, T.J. Patterns of spread in biological invasions dominated by long-distance jump dispersal: Insights from Argentine ants. *Proc. Natl. Acad. Sci. USA* **2001**, *98*, 1095–1100. [[CrossRef](#)]

34. Gippet, J.M.W.; Liebhold, A.M.; Fenn-Moltu, G.; Bertelsmeier, C. Human-mediated dispersal in insects. *Curr. Opin. Insect Sci.* **2019**, *35*, 96–102. [CrossRef]
35. Morrill, W.L. Dispersal of red imported fire ants by water. *Fla. Entomol.* **1974**, *57*, 39–42. [CrossRef]
36. Zhao, J.; Zhong, P.S.; Huang, T.; Zhang, S.S. Impact of precipitation on behavior of *Solenopsis invicta* Buren colony. *Chin. J. Vector Biol. Control* **2009**, *19*, 234–236.
37. Morrill, W.L. Overwinter survival of the red imported fire ant in central Georgia. *Environ. Entomol.* **1977**, *6*, 50–52. [CrossRef]
38. Quarles, A.; Kostecke, R.M.; Phillips, S.A. Supercooling of the red imported fire ant (*Hymenoptera: Formicidae*) on a latitudinal temperature gradient in Texas. *Southwest. Nat.* **2005**, *50*, 302–307. [CrossRef]
39. Vogt, J.T.; Smith, W.A.; Grantham, R.A.; Wright, R.E. Effects of temperature and season on foraging activity of red imported fire ants (*Hymenoptera: Formicidae*) in Oklahoma. *Environ. Entomol.* **2003**, *32*, 447–451. [CrossRef]
40. Drees, B.M.; Summerlin, B.; Vinson, S.B. Foraging activity and temperature relationship for the red imported fire ant. *Southwest. Entomol.* **2007**, *32*, 149–155. [CrossRef]
41. Potts, L.; Francke, O.; Cokendolpher, J. Humidity preferences of four species of fire ants (*Hymenoptera: Formicidae: Solenopsis*). *Insectes Sociaux* **1984**, *31*, 335–340. [CrossRef]
42. Tschinkel, W.R. The fire ant (*Solenopsis invicta*): Still unvanquished. In *Biological Pollution: The Control and Impact of Invasive Exotic Species*; Indiana Academy of Science: Indianapolis, IN, USA, 1993; pp. 121–136.
43. Vogt, J.T.; Wallet, B.; Coy, S. Dynamic thermal structure of imported fire ant mounds. *J. Insect Sci.* **2008**, *8*, 31. [CrossRef]
44. G-Econ 4.0 Dataset of Yale University. Available online: <https://gecon.yale.edu/> (accessed on 15 December 2019).
45. Gippet, J.M.; Mondy, N.; Diallo-Dudek, J.; Bellec, A.; Dumet, A.; Mistler, L.; Kaufmann, B. I'm not like everybody else: Urbanization factors shaping spatial distribution of native and invasive ants are species-specific. *Urban Ecosyst.* **2017**, *20*, 157–169. [CrossRef]
46. Human, K.G.; Weiss, S.; Weiss, A.; Sandler, B.; Gordon, D.M. Effects of abiotic factors on the distribution and activity of the invasive Argentine ant (*Hymenoptera: Formicidae*). *Environ. Entomol.* **1998**, *27*, 822–833. [CrossRef]
47. Buczkowski, G.; Richmond, D.S. The effect of urbanization on ant abundance and diversity: A temporal examination of factors affecting biodiversity. *PLoS ONE* **2012**, *7*, e41729. [CrossRef] [PubMed]
48. CliMond Climate Data. Available online: <https://www.climond.org/ClimateData.aspx> (accessed on 15 December 2019).
49. SRTM 90 m DEM Digital Elevation Database. Available online: <http://srtm.csi.cgiar.org/> (accessed on 15 December 2019).
50. Global Inventory Modeling and Mapping Studies. Available online: http://iridl.ldeo.columbia.edu/SOURCES/.UMD/.GLCF/.GIMMS/.NDVIg/.global/.dataset_documentation.html (accessed on 15 December 2019).
51. The Global Land Cover-SHARE (GLC-SHARE). Available online: <http://www.fao.org/land-water/land/land-governance/land-resources-planning-toolbox/category/details/en/c/1036355/> (accessed on 15 December 2019).
52. Travel Time to Major Cities: A Global Map of Accessibility. Available online: <https://forobs.jrc.ec.europa.eu/products/gam/index.php> (accessed on 15 December 2019).
53. Gridded Population of the World (GPW), v4. Available online: <https://sedac.ciesin.columbia.edu/data/collection/gpw-v4> (accessed on 15 December 2019).
54. The Nighttime Lights of the World Data Set. Available online: <https://sos.noaa.gov/datasets/nighttime-lights/> (accessed on 15 December 2019).
55. *Solenopsis invicta* Buren, 1972 in GBIF Secretariat. 2019. Available online: <https://www.gbif.org/species/5035230> (accessed on 15 December 2019).
56. AntWeb. Available online: <https://www.antweb.org/> (accessed on 15 December 2019).
57. CABI Invasive Species Compendium. Available online: <https://www.cabi.org/isc/datasheet/50569> (accessed on 15 December 2019).
58. Wetterer, J.K. Exotic Spread of *Solenopsis invicta* Buren (*Hymenoptera: Formicidae*) beyond North America. *Sociobiology* **2013**, *60*, 50–55. [CrossRef]
59. List of Administrative Areas for The Distribution of Agricultural Plant Quarantine Pests in China. 2019. Available online: http://www.gov.cn/zhengce/zhengceku/2019-10/19/content_5442299.htm (accessed on 15 December 2019).

60. Barbet-Massin, M.; Jiguet, F.; Albert, C.H.; Thuiller, W. Selecting pseudo-absences for species distribution models: How, where and how many? *Methods Ecol. Evol.* **2012**, *3*, 327–338. [CrossRef]
61. Elith, J.; Graham, C.H.; Anderson, R.P.; Dudík, M.; Ferrier, S.; Guisan, A.; Hijmans, R.J.; Huettmann, F.; Leathwick, J.R.; Lehmann, A. Novel methods improve prediction of species' distributions from occurrence data. *Ecography* **2006**, *29*, 129–151. [CrossRef]
62. Leathwick, J.; Elith, J.; Francis, M.; Hastie, T.; Taylor, P. Variation in demersal fish species richness in the oceans surrounding New Zealand: An analysis using boosted regression trees. *Mar. Ecol. Prog. Ser.* **2006**, *321*, 267–281. [CrossRef]
63. Buston, P.M.; Elith, J. Determinants of reproductive success in dominant pairs of clownfish: A boosted regression tree analysis. *J. Anim. Ecol.* **2011**, *80*, 528–538. [CrossRef]
64. Compton, T.J.; Morrison, M.A.; Leathwick, J.R.; Carabine, G.D. Ontogenetic habitat associations of a demersal fish species, *Pagrus auratus*, identified using boosted regression trees. *Mar. Ecol. Prog. Ser.* **2012**, *462*, 219–230. [CrossRef]
65. Elith, J.; Leathwick, J. Boosted Regression Trees for Ecological Modeling. R Documentation. 2017. Available online: <https://cran.r-project.org/web/packages/dismo/vignettes/brt.pdf> (accessed on 12 June 2011).
66. Elith, J.; Leathwick, J.R.; Hastie, T. A working guide to boosted regression trees. *J. Anim. Ecol.* **2008**, *77*, 802–813. [CrossRef]
67. R Core Team. *R: A Language and Environment for Statistical Computing*; R Core Team: Vienna, Austria, 2013.
68. Hijmans, R.J.; Phillips, S.; Leathwick, J.; Elith, J. *Dismo: Species Distribution Modeling, R Package Version 1.1–4*; R Core Team: Vienna, Austria, 2017; Volume 1.
69. Kuhn, M. Caret: Classification and Regression Training. ASCL 2015, ascl: 1505.003. Available online: <https://ascl.net/1505.003> (accessed on 15 December 2019).
70. Ridgeway, G.; Southworth, M.H.; RUnit, S. Package 'gbm'. *Viitattu* **2013**, *10*, 40.
71. Peterson, A.; Nakazawa, Y. Environmental data sets matter in ecological niche modelling: An example with *Solenopsis invicta* and *Solenopsis richteri*. *Glob. Ecol. Biogeogr.* **2008**, *17*, 135–144. [CrossRef]
72. Porter, S.D.; Tschinkel, W.R. Foraging in *Solenopsis invicta* (Hymenoptera: Formicidae): Effects of weather and season. *Environ. Entomol.* **1987**, *16*, 802–808. [CrossRef]
73. Ness, J.; Bronstein, J.L. The effects of invasive ants on prospective ant mutualists. *Biol. Invasions* **2004**, *6*, 445–461. [CrossRef]
74. Global Ecosystems and Environment Observation and Analysis Annual Report. 2019. Available online: <http://www.chinageoss.org/geoarc/2019/> (accessed on 15 December 2019).
75. De Blécourt, M.; Gröngroft, A.; Baumann, S.; Eschenbach, A. Losses in soil organic carbon stocks and soil fertility due to deforestation for low-input agriculture in semi-arid southern Africa. *J. Arid. Environ.* **2019**, *165*, 88–96. [CrossRef]
76. Yang, R.; Luo, Y.; Yang, K.; Hong, L.; Zhou, X. Analysis of forest deforestation and its driving factors in myanmar from 1988 to 2017. *Sustainability* **2019**, *11*, 3047. [CrossRef]
77. James, S.S.; Pereira, R.M.; Vail, K.M.; Ownley, B.H. Survival of imported fire ant (*Hymenoptera: Formicidae*) species subjected to freezing and near-freezing temperatures. *Environ. Entomol.* **2002**, *31*, 127–133. [CrossRef]
78. Xu, Y.-J.; Lu, Y.-Y.; Pan, Z.-P.; Zeng, L.; Liang, G.-W. Heat tolerance of the red imported fire ant, *Solenopsis invicta* (Hymenoptera: Formicidae) in mainland China. *Sociobiology* **2009**, *54*, 115.
79. Drees, B.M.; Berger, L.A.; Cavazos, R.; Vinson, B.S. Factors affecting sorghum and corn seed predation by foraging red imported fire ants (*Hymenoptera: Formicidae*). *J. Econ. Entomol.* **1991**, *84*, 285–289. [CrossRef]
80. Milks, M.; Fuxa, J.; Richter, A.; Moser, E. Multivariate analyses of the factors affecting the distribution, abundance and social form of Louisiana fire ants, *Solenopsis invicta*. *Insectes Sociaux* **2007**, *54*, 283–292. [CrossRef]
81. Whitcomb, W.; Bhatkar, A.; Nickerson, J. Predators of *Solenopsis invicta* queens prior to successful colony establishment. *Environ. Entomol.* **1973**, *2*, 1101–1103. [CrossRef]

Publisher's Note: MDPI stays neutral with regard to jurisdictional claims in published maps and institutional affiliations.



© 2020 by the authors. Licensee MDPI, Basel, Switzerland. This article is an open access article distributed under the terms and conditions of the Creative Commons Attribution (CC BY) license (<http://creativecommons.org/licenses/by/4.0/>).